**Climate
of the Past**
Open Access
Discussions

Late Holocene environmental reconstructions and the implications on flood events, typhoon patterns, and agriculture activities in NE Taiwan

L.-C. Wang[1], H. Behling[1], T.-Q. Lee[2], H.-C. Li[3], C.-A. Huh[2], L.-J. Shiau[4], and Y.-P. Chang[5]

[1]Department of Palynology and Climate Dynamics, Albrecht-von-Haller Institute for Plant Sciences, University of Göttingen, 37073 Göttingen, Germany
[2]Institute of Earth Sciences, Academia Sinica, Taipei, 128, Taiwan
[3]Department of Geosciences, National Taiwan University, Taipei, 106, Taiwan
[4]Institute of Applied Geosciences, National Taiwan Ocean University, Keelung, 202, Taiwan
[5]Department of Oceanography, National Sun Yat-sen University, Kaohsiung, 804, Taiwan

Correspondence to: L.-C. Wang (lwang6@uni-goettingen.de)
          and Y.-P. Chang (yuanpin.chang@mail.nsysu.edu.tw)

Abstract

In this study, we reconstructed the paleoenvironmental changes from a sediment archive of the floodplain lake in Ilan Plain of NE Taiwan on multi-decadal resolution for the last ca. 1900 years. On the basis of pollen and diatom records, we evaluated the record of past vegetation, floods, typhoons and agriculture activities of this area, which is sensitive to the hydrological conditions of the West Pacific. High sedimentation rates with low microfossil preservations reflected multiple flood events and humid climatic conditions during 100–1400 AD. A shortly interrupted dry phase can be found during 940–1010 AD. The driest phase corresponds to the Little Ice Age phase 1 (LIA1, 1400–1620 AD) with less disturbance by flood events, which enhanced the occurrence of wetlands (Cyperaceae) and diatom depositions. Humid phases with frequent typhoons are inferred by high percentages of *Lagerstroemia* and high ratios of planktonic/benthic diatoms, respectively, during 500–700 AD and Little Ice Age phase 2 (LIA2, 1630–1850 AD). The occurrences of cultivated Poaceae (*Oryza*) during 1250–1300 AD and the last ∼ 400 years, reflect agriculture activities, which seems to implicate strongly with the environmental stability. Finally, we found flood events which dominated during the El Niño-like stage, but dry events as well as frequent typhoon events happened during the La Niña-like stage. After comparing our results with the reconstructed proxy for tropical hydrological conditions, we suggested that the local hydrology in coastal East Asia were strongly affected by the typhoon-triggered heavy rainfalls which were influenced by the variation of global temperature, expansion of the Pacific warm pool and intensification of ENSO events.

1 Introduction

The western North Pacific tropical cyclones (TCs) can cause natural disasters associated with immerse economic and human losses for the East Asian coastal zones. High wind speeds, strong precipitations on land caused by TCs produce flood and landslide

disasters. According to the simulation from the recent 30 years typhoon data set, the factors that affected fluctuations of TCs were assumed. The strength of TCs is strongly associated with the tropical sea surface temperature (SST), and the global warming will lead to an upward trend in the TCs destructive potential (Emanuel, 2005). The paths of TCs are influenced by the cycle of El Niño–Southern Oscillation (ENSO) through the shifts of the main genesis region in the West Pacific (Elsner and Liu, 2003). During El Niño events, TCs formed further east with the northwesterly recurving path, while during La Niña years TCs moved straightly with a westerly path (Fig. 1). However, modern observed records of TCs are too short to reliably associate climate factors and the environmental changes for specific regions. According to previous studies in East Asia, the amount of precipitation is influenced by the variation of the summer monsoon and its correlation with solar insolation during Holocene (Liu et al., 2008; Qian et al., 2003; Varma et al., 2011; Wan et al., 2011; Zheng et al., 2013). Several studies suggest that the shifts of the northern limit of the ITCZ influenced the tropical hydrology then caused the drier Little Ice Age (LIA) on the East Asian continent (Hu et al., 2008; Zhang et al., 2008). This view has been challenged by findings of increased rainfall during the LIA in south China (Chen et al., 2005; Chu et al., 2002) and Taiwan (Chen et al., 2009; Wang et al., 2011, 2013). Such spatial variations in precipitation reflect the regional characteristics of climate, such as the monsoonal precipitation or TCs-triggered heavy rainfall. However, studies on influences of the intensity and frequency of TCs to local hydrology during the Holocene are rare (Chen et al., 2012; Wang et al., 2013; Woodruff et al., 2009), even though the hydrological conditions, especially flooding, at the East Asian coast were strongly affected by the TCs.

Ilan Plain, which locates in northeastern part of Taiwan, is situates under the main paths of TCs from the West Pacific (Fig. 1). It is an ideal area for the paleo-typhoon study, but very little investigation has been done so far despite its importance (Chen et al., 2012). In addition, the interaction between human–environment is a priority question in paleoecology. Lin et al. (2007) found that the archeological hiatus in Ilan Plain during the late Holocene may correlate to frequent typhoons and landslides, but direct

evidence and precisely duration of agriculture activities are lacking. Therefore, in this study we will use the pollen and diatom records of high-resolution lake sediments to detect the typhoon patterns and anthropogenic impacts on NE Taiwan during the late Holocene. We will assess the role of frequent nature hazards on settlements during the past. Furthermore, we will compare our data with main paleoclimatology proxies, which influence the precipitation in Ilan Plain to reveal their relations to the typhoon pattern at the West Pacific coastal zones.

2 Study area

The study area, Ilan Plain, is located at the northeastern coast of Taiwan and enclosed by steep mountains (Fig. 1). Only the eastern part is open and faces to the North Pacific. The east coast is scatted by sand dunes, where the rivers are impeded. Flooding is frequent in low elevated areas during the heavy rain days. The plain is an alluvial fan with extremely high accumulation rate. The main source of the alluvium is the denudation from the mountain region among Lanyang River system (Letouzey and Kimura, 1986). The superficial rocks of surrounding mountains consist of metasandstone, shale, and slate, while the alluviums of the plain are the mixture of stone, sand, silt, and clay.

The Ilan Plain belongs to the subtropical monsoon region. The climate is warm and humid. The Ilan Weather Station (24°45′56″ N, 121°44′53″ E, 7.2 m a.s.l.), reports a mean annual mean temperature of 22.5 °C from data collected since 1981 to 2010. The mean annual precipitation is 2238 mm (Fig. 2). The extremely humid months are September, October and November with precipitation rates more than 300 mm. The autumn rainfall maximum during the annual cycle can be correlated to the late-season typhoon events and transient disturbances embedded in the northeasterly monsoon flow during the passage of cold fronts (Chen and Chen, 2003). The dry season is unclear, because of the influences of winter monsoon, which is characterized by northeasterly

Title Page

Abstract | Introduction

Conclusions | References

Tables | Figures

|◀ | ▶|

◀ | ▶

Back | Close

Full Screen / Esc

Printer-friendly Version

Interactive Discussion

wind with cold and wet air blown from the North Pacific that is originated from the Mongolia Plateau (Fig. 1).

The vegetation of the lowland and hills of Ilan Plain is assigned to the subtropical evergreen rain forest zone (Su, 1984), although the most plain area have been reclaimed for rice paddy. In the riverine or alluvial fan areas, *Alnus formosana*, *Barringtonia racemosa*, and *Cephalanthus naucleoide* are scattered. Poaceae, Cyperaceae are dominated in the coastal marshland (Lin et al., 2007). According to the modern vegetation map of Taiwan (Fig. 1) (Chiou et al., 2009), the zonation of forests in the surrounding mountains as well as the drainage basin of Lanyang River is strongly influenced by altitude. *Machilus thumnbergii*, *Castanopsis cuspidate*, *Lagerstroemia subcostata*, *Adisia sieboldii* are important and common woody trees in the lower montane evergreen broad-leave forests (LMF, < 1200 m a.s.l.). *Cyclobalanopsis morri*, *Pinus taiwanensis*, *Alnus formosana* are the main species in montane mixed needle-broad-leave forests (MF, 1200–2200 m a.s.l.). The upper montane needle-leave forests (UMF, >2200 m a.s.l.), are dominated by *Tsuga chinensis* var. *formosana*, and *Abies kawakamii*.

Dahu Lake (DHL) is located on the northwestern margin of the Ilan Plain (Fig. 1). DHL is a lowland lake (17 m a.s.l.) with the average water depth of 2 m and a surface area of about 10.6 ha. The lake is isolated and the primary water inputs are from rainfall, the surface runoff of the catchment, and the groundwater discharges. Lanyang River is the main river of the plain, and locates in the south of DHL. The previous study addressed the high sedimentation rates of DHL as a consequence of massive inputs of suspended material from overflows of the Lanyang River at various time intervals during the middle to late Holocene (Chen et al., 2012).

Title Page

Abstract | Introduction

Conclusions | References

Tables | Figures

|◀ | ▶|

◀ | ▶

Back | Close

Full Screen / Esc

Printer-friendly Version

Interactive Discussion

3 Materials and methods

3.1 Coring and radiocarbon dating

A 35 m sediment core (DH-7B) was taken and reached to the bottom by using stainless corer on a floating platform in the western area of DHL at January 2008. The sediment core was stored at 4 °C in a dark room. The core was subsampled at 1 cm intervals for pollen and diatom analysis.

The sediments of core DH-7B are mainly consisted of gray clay, and interrupted with 10- to 70-cm-thick-layers of sand, silt, and brown clay throughout the upper 1400 cm (Fig. 3). Sand layers are presented at the depth of 790–800, and 650–690 cm, while the silt layers are occurred at the depth of 720–740, 690–700, and 460–480 cm. The brown clay layers are only found at the depth of 440–460 cm and upper 70 cm.

Chronologies of the core were determined by ^{210}Pb and AMS ^{14}C dating. For ^{210}Pb, 10 samples taken from the upper 25 cm of the core were analyzed for ^{210}Po by α-spectrometry, with ^{209}Po added as the yield determinant. More detailed procedures can be found in Huh and Su (2004). Radiocarbon dates were performed by accelerator mass spectrometry at the Rafter Radiocarbon Laboratory in New Zealand (Chen et al., 2012). Radiocarbon carbon ages were calibrated using CALIB Rev 6.0.2 (Stuiver et al., 2005). The age model of this study was carried out on the basis of linear interpolation of dates of four ^{14}C dates and the ^{210}Pb dates.

3.2 Pollen and diatom analysis

For the extraction of pollen and diatoms, subsamples at 5–20 cm intervals (0–300 cm core depth at 5 cm intervals; 300–900 cm at 10 intervals; 900–1100 cm at 20 cm intervals) were used. The samples with low preservations of pollen or diatom which counted less than 100 pollen grains or diatom valves were discarded after microscope examination. Below 1100 cm core depth, samples were not analyzed because of poor preservation of both microfossils.

The pollen extraction was treated following dense media methods (Nakagawa et al., 1998). Five gram of dry weight sediment were digested with 36 % HCl, 10 % NaOH, rinsed with distilled water 6–20 times repeatedly. After that, samples were concentrated using dense-media (solution of density 1.88) and treated with acetolysis. One tablet with a given number of *Lycopodium* spores was added to each sample before chemical treatments to determine the concentration. Pollen identification and counts were done with a 400 × optical microscopy. With the help of pollen and spores flora of Taiwan (Huang, 1972, 1981), pollen grains were identified to the lowest taxonomic level. For most samples, 300 pollen grains were counted. Percentages are based on the total pollen sum. Fern spores and the green algae *Pediastrum* were not included, but presented as the percentages of the sum of all pollen.

On the basis of the modern vegetation map, the main tree pollen types were assigned into three groups, upper mountain forest (UMF), mountain forest (MF), and lower mountain forest (LMF), that either corresponds to different vegetation in the neighbour mountains. The herbaceous pollen types were attributed to two groups by the habitats as either terrestrial (non-arboreal pollen, NAP) or aquatic types (wetland). The Poaceae pollen with a long axis of more than 40 μm was identified as cultivated Poaceae (Itzstein-Davey et al., 2007), although other authors used 35 μm as a separation criterion between cultivated and wild Poaceae (X. Wang et al., 2010).

Diatom analysis is mainly followed the way described by Wang et al. (2013). Half gram of dry weight sediment was digested with 32 % H_2O_2 and 10 % HCl, then mounted on slides using mounting media (Wako). 300 diatom valves were identified and counted under 1000 × optical microscopy. The identification of diatom species and their ecological interpretation is based on Freshwater Diatom Flora of Taiwan and collecting references therein (Charles, 1985; Krammer and Lange-Bertalot, 1986; L. C. Wang et al., 2010; Wu et al., 2011). Thus, all diatom species were attributed to groups that correspond to preferred habitat types (planktonic, epiphytic, and benthic).

Late Holocene environmental reconstructions in NE Taiwan

L.-C. Wang et al.

3.3 Data analysis

In order to mitigate the effect of rare taxa that poorly explain the complete trend of vegetation, only pollen taxa which occurred with a percentage value lager than 3 % in at least 3 samples were included in the numerical analyses. The stratigraphic diagram were conducted using Tilia and Tiliagraph (Grimm, 1993) and C2 program (version 1.5 for Windows) (Juggins, 2005). Pollen data were subjected by cluster analysis using the Edwards and Cavalli-Sforza's chord distance measure of CONISS in TGView to define the zonation.

The ordination analyses and plotting were carried by using software for Windows 4.5 and CanoDraw for Windows 4.13 (Ter Braak and Smilauer, 2002). Pollen percentages were square-root-transformed for the numerical analyses in order to removing the affect from dominant taxa and optimizing the signal-to noise ratio (Jantz and Behling, 2012; Wang et al., 2014). Detrended correspondence analysis (DCA) yielded the length of the environmental gradients with the value 1.61 of standard deviation (SD). Thus, a linear ordination method (principle component analysis, PCA) is appropriate for these data sets (Birks and Birks, 1998).

4 Results

4.1 Stratigraphy and chronology

The upper 1100 cm core sediments are mainly composite of mineral content. Only sediment depths at 460–440 cm and uppermost 70 cm have organic enriched brown clay, while the rest of core sediments are consist of organic-poor clay, silt and fine sand (Fig. 3).

Four radiocarbon dates and ^{210}Pb-derived sedimentation rate of the upper 23.5 cm were used to create an age model of the core DH-7B. The results of radiocarbon dating have no reversal in ages, suggesting a continued and undisturbed deposition

environment (Table 1). According to the age model, the upper 1100 cm of the core represented the records for the period of 100 to 2007 AD (Fig. 3).

Sedimentation rates are not consistent, and have higher values at the lower part of depth from 1000–130 cm (100–1400 AD) with values ranging from 0.74–0.71 cm yr^{-1}. Above the depth of 130 cm (1400–2007 AD), sedimentation rates decline to the relatively low values of 0.35–0.16 cm yr^{-1}. On the basis of the sedimentation rate and samples interval, the time resolution of our proxies can attend to 20–25 years in resolution over the last two millennia.

4.2 Pollen and diatom results

Due to the extremely poor preservation of microfossils in some samples, only 109 samples were used for pollen analysis and 35 samples for diatom analysis. To clarify the analysis, four local pollen zones (LPZ) were identified through the visual examination to crucial variations of pollen assemblages, lithostratigraphy, and the CONISS dendrogram (Fig. 4). The assemblages of pollen and diatom have somehow coherent variations in core DH-7B (Fig. 5), which both shown higher concentrations and component variations in organic-rich layers (Fig. 6). The resemblance in trends enables the diatom assemblages to be assigned into four pollen zones at the same depths with pollen assemblages.

LPZ 1 (core depth: 1100–440 cm; age: 100–1010 AD) has higher sedimentation rate (0.71 cm yr^{-1}) with low preservation of pollen and diatoms. Arboreal pollen (AP) comprises 72 % of the total pollen. UMF and MF pollen are the dominant pollen types, and *Pinus* is the most important taxa, which is averaging about 30 % of the pollen sum. The pollen preservation is extremely low, and the sediments consist of coarse silt and sand at the depths between 700–650 cm. However, LMF pollen *Lagerstroemia* has a maximum value of 76 % at the depth of 665 cm. In the upper part of the core, sediments consist of silt and organic-rich brown clay at depths of 480–440 cm, wetland pollen such as Cyperaceae, LMF pollen and riverine pollen *Barringtoniai* are increased. Fern

spores are dominated, with average value of 225. Diatoms only presents at the end of the zone with the dominance of benthic diatoms (Fig. 5).

LPZ 2 (core depth: 460–130 cm; age: 1010–1400 AD) is characterized with poor preservation of diatoms and relatively high sedimentation rates (0.74 cm yr^{-1}). Pollen concentration remains low. AP has 67 % of the pollen sum with dominated of UMF and MF pollen. *Pinus* declines slightly to 24 % in average. *Alnus* pollen becomes more important, and is averages of 12 %. The percentages of UMF pollen *Abies* and *Tsuga* are slightly higher than in Zone LPZ1. Percentages of Poaceae are much higher, especially in the middle part of the zone. Fern spores are slightly decreased, and the mean value is 205.

In LPZ 3 (core depth: 130–70 cm; age: 1400–1620 AD), the sedimentation rate declines from 0.35 to 0.16 cm yr^{-1}. The concentrations of pollen are much higher, but vary remarkably. With a marked decrease of UMF and MF pollen, AP decreases to 38 %, although the LMF pollen varies little. *Barringtonia* is almost absent. Cyperaceae is the most important taxa, with averaging of 36 %. Fern spores are reduce (∼ 183). Diatom concentrations increase and epiphytic diatoms dominate the assemblages.

In LPZ 4 (core depth: 70–0 cm; age: 1620–2007 AD), the sedimentation rate remains low and increases slightly during the last centuries. The concentrations of pollen are high. AP is about 48 % of the total pollen. *Castanopsis* is the dominated tree taxa, even though comparing with the percentages of the other LMF taxa. Pollen values of *Ardisia*, *Liquidambar*, *Lagerstroemia* are low. The zone is characterized by the increase of anthropogenic pollen, including wild and cultivated Poaceae, Asteraceae and *Artemisia*. Cyperaceae pollen remains low (∼ 7 %). Fern spores decrease markedly, and the mean value is 39. Percentages of green algae *Pedistrum* peaks at the end of the zone and reaches the value of 116. Diatom concentrations are much higher than in LPZ 3 and occur consistently throughout the zone. Planktonic diatoms and larger epiphytic diatoms, *Cymbella tumida*, *Encyonema mesianum*, *Epithemia sorex*, and *Ulna ulna* show an increase trend during the lower part of the zone. Percentages of benthic diatoms such as

Title Page

Abstract | Introduction

Conclusions | References

Tables | Figures

◄ | ►

◄ | ►

Back | Close

Full Screen / Esc

Printer-friendly Version

Interactive Discussion

Staurosira construens remain low at the beginning of the zone, but increase gradually towards the top.

4.3 Principal Component Analysis

The PCA results of pollen data show important ordinations of data set, revealing the relationships between samples and pollen taxa (Fig. 6). The eigenvalues are 0.30 for the axis of first component (PC1) and 0.20 for the axis of second component (PC2). Along the axis of PC1, Poaceae and cultivated Poaceae represent the negative scores and correspond best to LPZ 4. Along the axis of PC2, all taxa of UMF and MF have negative scores with good correlation to LPZ 1 and LPZ 2, while the Cyperaceae have the highest positive scores with the somehow correlation to LPZ 3.

5 Discussion

5.1 Evaluation of proxies

The Dahu Lake (DHL) is mainly surrounded by quartz-rich sandstone and argillite, while the sediments with high amounts of illite and muscovite are mainly from the upstream of the adjacent Lanyang River (Fig. 6), where outcrop is consists of 30 % illite and muscovite. Thus, the increase of illite and muscovite in the sediment core can be seen as proxy of overflow of the Lanyang River (Chen et al., 2012), which transports numerous inorganic clay into DHL and dilutes the concentrations of pollen and diatoms. Xu et al. (1996) found that pollen compositions had a markedly difference between the alluvial and lacustrine sediments on the basis of a surface sediment studied in the North China Plain. The lacustrine sediments are characterized by high pollen concentration, while the alluvial sediments are characterized by more mountainous pollen and high variations of pollen taxa in different depositional faces. Therefore, the low concentration of pollen grains during LPZ 2 and LPZ 1 can be correlated to the numerous inputs of alluvium.

Palynological data form lake sediments had been broadly used to indicate the variations of paleovegetation within the pollen source area, from which most of the pollen grains originate (Sugita, 1993; Prentice, 1985). Due to the high hydrological dynamics and the geomorphic complexity of the fluvial plain, the pollen grains of lake can be contributed to the deposition of airborne pollen from local vegetation (LMF) and transportation from sources throughout the river drainage system (Brown, 1985; Chmura and Liu, 1990). According to the variations of pollen and diatom concentrations, the fluvial transport is dominated in LPZ 1 and LPZ 2 with UMF and MF pollen, especially *Pinus*. However, the distances between DHL and the nearby *Pinus* forest is more than 10 km (Fig. 1). For explaining this, we assumed that the markedly high occurrence of *Pinus* pollen (more than 30 %) in DHL was attributed to the overflows of rivers. Although the pollen assemblage of river transport have used for indicating to the vegetation history in river drainage area (Kröpelin et al., 2008). The variations and percentages of *Pinus* in DHL are much higher than the records in Yuanyang Lake (Chen and Wu, 1999), which is locates at the Lanyang River drainage area, and the coast sites of Iland Plain (Lin et al., 2007) during the last 2000 years. Therefore, we assume that the higher percentages of UMF and MF pollen are due to resuspension of river deposits, corresponding to river flood stages, rather than the forest development in the catchment area. Next, we combined this assumption with PCA analysis. The axis of PC2 reveals the strong negative correlation with UMF and MF pollen, and fit well to LPZ 1 and LPZ 2, suggesting the axis of PC2 from the pollen data is a good indicator for the flood intensity.

Percentage of *Lagerstroemia* reaches to 78 % in the middle part of LPZ 1. The results are much higher than the palynological records in the lowland Ilan Plain, which the percentage of *Lagerstroemia* varies below 10 % (Lin et al., 2007). In addition, the grain size, indicator of the input from the local watershed, shows a synchronic increase with *Lagerstroemia* (Fig. 6). The large deciduous tree, *Lagerstroemia subcostata* is common in low latitude forests of the surrounding mountains in the Ilan Plain. These inputs can be attributed to the typhoon-triggered local landslides and heavy rainfalls,

which eroded the soil from *Lagerstroemia* forests then transported it into DHL (Chen et al., 2012). The anomaly of *Lagerstroemia* percentages (> 20 %) has been assumed as a signal of strong (or frequent) typhoon events.

Distinct changes in the distribution of diatom assemblage within a lake can be related to changes in the aquatic conditions, and the ratio of benthic and planktonic diatoms (P/B ratios) has been used to infer past fluctuations of lake level and precipitation (Laird et al., 2011). On the basis of this assumption, the variation of P/B ratios in our study is used as the proxy of paleo-precipitations.

In Taiwan, the cultivated Poaceae (Oryza) have been used as a proxy of agriculture activities (Tsukada, 1967), while the wood of *Lagerstroemia* is an important burning material for ancient agriculture activity processing by native people. The axis of PC1 of the pollen data reveals a strong negative relation with wild and cultivated Poaceace but a positive relation with *Lagerstroemia*. As such result, the pollen-PC1 as well as the percentage of cultivated Poaceae is considered to indicate the signals of agriculture activities.

5.2 Interpretation of paleoclimate and their impacts on agriculture activates

According to the pollen and diatom records, environmental changes are reconstructed. The following discussion interprets the implications of the proxies presented for each zone and the extent to which DHL records reflect the fluvial plain evolution, climate changes, and the traces of agriculture activates during the last 1900 years.

LPZ 1 (100–1010 AD) corresponds to pre-Medieval Warm Period (pre-MWP) and is characterized by high sedimentation rate and extremely low pollen concentration along with poor diatom preservation. The high negative values of pollen-PC2 along with high percentages of illite and muscovite reflects numerous inputs from the overflow of Langyang Rivers, indicating that the DHL experienced frequent floods and reflecting the humid climate condition during the period. The floodplain landscape with the meandering river systems is intensified by the synchronic increase of riverbank shrub, *Barringtonia* in the sediment cores of DHL and coastal area (Lin et al., 2007). During

Late Holocene environmental reconstructions in NE Taiwan

L.-C. Wang et al.

Title Page

Abstract | Introduction

Conclusions | References

Tables | Figures

◁ | ▷

◁ | ▷

Back | Close

Full Screen / Esc

Printer-friendly Version

Interactive Discussion

500–700 AD, the high percentages of *Lagerstroemia* and plentiful coarse sediments infers to the torrential precipitation triggered by TCs (Chen et al., 2012). The decrease of pollen-PC2 and the increase of microfossil concentrations reflect drier climatic conditions with either less or weaker flood events during 940–1010 AD. The landscape of DHL temporally turns out to be a shallow lake surround with sedges, which indicates by the dominance of benthic diatoms and Cyperaceae pollen. The high positive values of pollen-PC1 and low percentages of cultivated Poaceae imply little human impacts at the study area. This assumption is strengthened by the hiatus of the archaeological records in Inlan during 450 BC–650 AD (Lin et al., 2004, 2007). Combining with the paleoenvironmental changes, the gap in the archaeological record can be corresponded to frequent nature hazards, such as floods and TCs during this period.

LPZ 2 (1010–1400 AD) corresponds to the Medieval Warm Period (MWP) and is characteristics with higher sedimentation rate as well as low preservation of pollen and diatoms. This indicates to the input from overflow of rivers and suggests a high flooding frequency and humid climatic conditions. Pollen PC-2 decreases gradually (more negative) but varies little, inferring the stable hydro-environment with increasing rainfall. The increase of sedimentation rate in South Okinawa Trough (SOT) (Fig. 1) implies more fluvial material inputs and suggests wetter climate conditions in this period (Fig. 6).

During this period, human disturbance of forest is confirmed by a rapid increase of pioneer forest, *Alnus*, *Mallotus* and a correspondence decline in ethnobotanical plant, *Lagerstroemia*. Agriculture activities were indicted by the occurrences of cultivated Poaceae, and the increasing frequency of disturbance indicators, Poaceae, Asteraceae, and *Artemisia*. The anthropogenic proxy pollen-PC1 is indicating a clear agriculture period during 1250–1300 AD. The results are confirmed by archaeological records, which found that agriculture in the study area was established in alluvial fans, riverine and littoral areas from around 1250 AD (Liu, 2000). During 1300–1400 AD, the intense flood events, inferred by pollen-PC2, may correlate to the decline of agriculture activities.

Important characteristics of LPZ 3 (1400–1620 AD, corresponding to the Little Ice Age 1 (LIA1)), are marked by the decline of sedimentation rates. The better preservation of pollen grains and diatom valves along with the high values of pollen-PC2 suggest that the DHL is little affected by the overflow of rivers. The marked decrease of high latitude pollen, mainly *Pinus*, and the disappearance of riverine taxa *Barringtonia,* indicate the reduction of flood events. The weaker capability of fluvial materials transportation is confirmed by the decrease of the sedimentation rate of the core in SOT (Fig. 7) (Li et al., 2011), and is refers to the drier climate in NE Taiwan. The continuously high percentages of Cyperaceae pollen and epiphytic diatoms reflect that the vicinity of DHL is expanded wetlands with sedges. The human activities are reduced during this period. The weak agriculture activities are indicated by low concentration of cultivated Poaceae and pollen-PC1.

LPZ 4 (1620–2007 AD, corresponding to Little Ice Age 2 (LIA2) toward modern situation), is characterized by changes of sediment contents from mineral clay to organic-rich clay, inferring that the DHL is out of the range of floodplain, which is influenced by overflows of rivers, mainly caused by Lanyang River. During this period, the hydrological conditions of DHL are similar with today, which is an enclosed lake without influences of alluviums. Although the flood variations cannot be reflected by the proxy of overflows, such as pollen-PC2, the variations of diatom assemblages imply to indicate the changes of lake level. The ratio of planktonic and benthic diatoms (P/B) and the values of grain size increase during the duration of 1620–1850 AD (LIA 2), reflecting extremely rainfalls at this stage (Fig. 6). The extremely rainfalls in NW Taiwan during LIA2 are also inferred by the increase of diatom-derived pH proxy in the subalpine lake of NE Taiwan (Wang et al., 2013) and the increase of freshwater diatoms in marine sediment of SOT (Fig. 8). Therefore, the occurrences of frequent TCs in NW Taiwan during LIA 2 are exanimated.

The increase of cultivated Poaceae with high negative values of pollen-PC1, suggests that the agriculture activities occurred throughout the last four centuries. The higher nutrient level of lakes due to human activities is implied by the increase of

Myriophyllum pollen (Grace and Wetzel, 1978) and the green algae *Pediastrum* (Weckström et al., 2010). According to the historical literature, Han Chinese moved into the northern Ilan Plain then built up the irrigation systems for paddy-field-farming in 1796 AD. The clear increasing trend of cultivated Poaceae after 1800 AD may correlate to the irrigated agriculture of Han Chinese, which increases the production and cultivated area of rice (Fig. 7).

5.3 Hydrologic variability in the East Asian coast and its relation with warm pool and ENSO

We compared the reconstructions of flood intensity and typhoon frequency of DHL with the main factors of hydrological variations in West North Pacific, including variations of ENSO (Yan et al., 2011b), Indo-Pacific Warm Pool (IPWP) (Oppo et al., 2009), East Asia Summer Monsoon (EASM) (Wang et al., 2005), East Asia Winter Monsoon (EAWM) (Yancheva et al., 2007), and the north-south migration of ITCZ (Yan et al., 2011a) during the last two millenniums (Fig. 9). The flood events seem to positively correlate with SST of IPWP, but are weakly correlated to the variations of EASM, EAWM and ITCZ. The rainfall, which is influenced by the intense strengths of winter and summer monsoon or the shifts of ITCZ, generally is not high enough to trigger flood event in coastal East Asia. The flood events in Ilan Plain are mainly caused by heavy autumn rain, which is induced by the circulation of typhoon and the co-movement effect of winter monsoon (Fig. 2). Therefore, we suggest that the strengths and the seasonality of the TCs are the main factors causing the flood events at this region. IPWP is the largest reservoir of warm surface water on the Earth and the main source of heat and moisture of atmosphere. The small variations of SST impact the location and strength of convection of the Hadley and Walker circulations, and influence global atmospheric circulation and tropical hydrology (Barsugli and Sardeshmukh, 2002; Oppo et al., 2009). When warmer SST occurs in the equatorial eastern Pacific Ocean, TCs tend to occur at the middle part of the equatorial Pacific. Therefore, the warmer SST of IPWP may increase the intensity of typhoons generated in West Pacific Warm Pool, and caused

flood events during pre-MWP and MWP, and vice versa. Our results also suggest that the variations of global temperature correlate to the strength of TCs, which is intense in MWP and is weak in LIA1 (Emanuel, 2005).

It is worthy to note that the flooding events dominate the record during the El Niño-like stage, but dry events as well as frequent typhoons both happened during the La Niña-like stage (Fig. 9). Chen et al. (2012) highlighted TCs chiefly landfall in Taiwan and south China during the La Niña-like stage, because the tracks of typhoon are highly influenced by the ENSO (Fogarty et al., 2006; Huang and Xu, 2010). However, this assumption cannot explain why the dry events (less flood events) also occurred in pre-MWP and LIA1 during the La Niña-like stage. The statistic study of 50-years typhoon records in Fujian (Fig. 1) reveals that the number of heavy rain days is increased during El Niño years, although the number of TCs affecting Fujian in general is higher during La Niña years (Yin et al., 2010). Therefore, due to the less heavy rain days, the flood events are decreased during the moderate La Niña-like stage, but the numbers of typhoon-induced landfalls on coastal region of East Asia are increased to the maximum during the strong La Niña-like stage.

6 Conclusions

The analysis of the DHL sediment core derived from the floodplain in NE Taiwan provides a multi-decadal record of hydrological variations and the clear evidence of agriculture activities during last two thousand years. The used proxies in this study for paleofloods (pollen-PC2) and agriculture activities (pollen PC-1), which are implied by the PCA results, the high percentages of *Lagerstroemia* pollen, and the increase of diatom P/B ratios are used to indicate frequent typhoon events. The globally warm period during 100–1400 AD (Pre-MWP, MWP) is characterized by high sedimentation rates and low microfossil preservations, inferring the strong influences caused by overflow of the rivers. *Pinus* pollens, which are unearthed from the flooding sediments, are the most abundant compositions of this stage. This finding reflects that multiple flood events and

humid climate are common during this period. A short interruption of dry event has been found during the period of 940–1010 AD, as well as the frequent typhoon events occurred during the duration of 500–700 AD. The globally cool period, LIA1 is found in our record, inferring to the shift of dry climatic conditions accompanying with less flood events discovered at 1400 AD. At the same time, wetland pollen, Cyperaceae, and epiphytic diatoms dominates the records. The climatic conditions change to more humid due to the intense of typhoon frequency during 1630–1850 AD, which is dominated by planktonic diatoms. The increased impact of human agriculture activities are recorded during the ages of 1250–1300 and the last ∼ 400 years. It seems to be associated strongly with stable environment and climate. On the basis of the comparisons with reconstructed proxy of warm pool, ENSO, monsoon, and ITCZ, the local hydrology of the coastal region of Taiwan is strongly affected by the typhoon-triggered heavy rainfalls, which are influenced by the variation of global temperature, expansion of warm pool and the intensification of ENSO events, rather than the seasonal precipitations, which are influenced by the EASM, EAWM or the shift of the ITCZ.

References

Barsugli, J. J. and Sardeshmukh, P. D.: Global Atmospheric Sensitivity to Tropical SST Anomalies throughout the Indo-Pacific Basin, J. Climate, 15, 3427–3442, doi:10.1175/1520-0442(2002)015<3427:GASTTS>2.0.CO;2, 2002.

Brown, A. G.: The potential use of pollen in the identification of suspended sediment sources, Earth Surf. Proc. Land., 10, 27–32, doi:10.1002/esp.3290100106, 1985.

Charles, D. F.: Relationships between surface sediment diatom assemblages and lakewater characteristics in Adirondack Lakes, Ecology, 66, 994–1011, 1985.

Chen, C. S. and Chen, Y. L.: The rainfall characteristics of Taiwan, Mon. Weather Rev., 131, 1323–1341, 2003.

Chen, H.-F., Wen, S.-Y., Song, S.-R., Yang, T.-N., Lee, T.-Q., Lin, S.-F., Hsu, S.-C., Wei, K.-Y., Chang, P.-Y., and Yu, P.-S.: Strengthening of paleo-typhoon and autumn rainfall in Taiwan corresponding to the Southern Oscillation at late Holocene, J. Quaternary Sci., 27, 964–972, doi:10.1002/jqs.2590, 2012.

Chen, J., Wan, G., Zhang, D. D., Chen, Z., Xu, J., Xiao, T., and Huang, R.: The "Little Ice Age" recorded by sediment chemistry in Lake Erhai, southwest China, Holocene, 15, 925–931, doi:10.1191/0959683605hl863rr, 2005.

Chen, S. H. and Wu, J. T.: Paleolimnological environment indicated by the diatom and pollen assemblages in an alpine lake in Taiwan, J. Paleolimnol., 22, 149–158, 1999.

Chen, S. H., Wu, J. T., Yang, T. N., Chuang, P. P., Huang, S. Y., and Wang, Y. S.: Late Holocene paleoenvironmental changes in subtropical Taiwan inferred from pollen and diatoms in lake sediments, J. Paleolimnol., 41, 315–327, 2009.

Chiou, C.-R., Chen, T.-Y., Liu, H.-Y., Wang, J.-C., Yeh, C. L., and Hsieh, C.-F.: Modern vegetation map of Taiwan, Forestry Bureau, Council of Agriculture Executive Yuan, R. O. C. Taiwan, Taipei, 2009.

Chmura, G. L. and Liu, K.-B.: Pollen in the lower Mississippi River, Rev. Palaeobot. Palynol., 64, 253–261, doi:10.1016/0034-6667(90)90140-E, 1990.

Chu, G., Liu, J., Sun, Q., Lu, H., Gu, Z., Wang, W., and Liu, T.: The "Mediaeval Warm Period" drought recorded in Lake Huguangyan, tropical South China, Holocene, 12, 511–516, doi:10.1191/0959683602hl566ft, 2002.

Elsner, J. B. and Liu, K. B.: Examining the ENSO-typhoon hypothesis, Clim. Res., 25, 43–54, 2003.

Late Holocene environmental reconstructions in NE Taiwan

L.-C. Wang et al.

Title Page

Abstract | Introduction

Conclusions | References

Tables | Figures

|◄ | ►|

◄ | ►

Back | Close

Full Screen / Esc

Printer-friendly Version

Interactive Discussion

Emanuel, K.: Increasing destructiveness of tropical cyclones over the past 30 years, Nature, 436, 686–688, doi:10.1038/nature03906, 2005.

Fogarty, E. A., Elsner, J. B., Jagger, T. H., Liu, K., and Louie, K.: Variations in typhoon landfalls over China, Adv. Atmos. Sci., 23, 665–677, doi:10.1007/s00376-006-0665-2, 2006.

Grace, J. and Wetzel, R.: The production biology of Eurasian watermilfoil (*Myriophyllum spicatum* L.): a review, J. Aquat. Plant Manage., 16, 1–11, 1978.

Grimm, E.: TILIA: A Pollen Program for Analysis and Display, Ill. State Mus, Springf., IL, 1993.

Hu, C., Henderson, G. M., Huang, J., Xie, S., Sun, Y., and Johnson, K. R.: Quantification of Holocene Asian monsoon rainfall from spatially separated cave records, Earth Planet. Sc. Lett., 266, 221–232, doi:10.1016/j.epsl.2007.10.015, 2008.

Huang, F. and Xu, S.: Super typhoon activity over the western North Pacific and its relationship with ENSO, J. Ocean Univ. China, 9, 123–128, doi:10.1007/s11802-010-0123-8, 2010.

Huh, C.-A. and Su, C.-C.: Distrribution of fallout radionuclides (^{7}Be, ^{137}Cs, ^{210}Pb and ^{239,240}Pu) in soils of Taiwan, J. Environ. Radioact., 77, 87–100, 2004.

Itzstein-Davey, F., Atahan, P., Dodson, J., Taylor, D., and Zheng, H.: A sediment-based record of Lateglacial and Holocene environmental changes from Guangfulin, Yangtze delta, eastern China, Holocene, 17, 1221–1231, doi:10.1177/0959683607085128, 2007.

Jantz, N. and Behling, H.: A Holocene environmental record reflecting vegetation, climate, and fire variability at the Páramo of Quimsacocha, southwestern Ecuadorian Andes, Veg. Hist. Archaeobot., 21, 169–185, doi:10.1007/s00334-011-0327-x, 2012.

Juggins, S.: C2 Version 1.5: software for ecological and palaeoecological data analysis and visualisation, University of Newcastle, Newcastle, 2005.

Krammer, K. and Lange-Bertalot, H.: Süswasserflora von Mitteleuropa: Bacillariophyceae, Stuttg. Gustav Fish., Germany, 1–4, 1986.

Kröpelin, S., Verschuren, D., Lézine, A.-M., Eggermont, H., Cocquyt, C., Francus, P., Cazet, J.-P., Fagot, M., Rumes, B., Russell, J. M., Darius, F., Conley, D. J., Schuster, M., von Suchodoletz, H., and Engstrom, D. R.: Climate-driven ecosystem succession in the Sahara: the past 6000 years, Science, 320, 765–768, doi:10.1126/science.1154913, 2008.

Laird, K. R., Kingsbury, M. V., Lewis, C. F. M., and Cumming, B. F.: Diatom-inferred depth models in 8 Canadian boreal lakes: inferred changes in the benthic : planktonic depth boundary and implications for assessment of past droughts, Quaternary Sci. Rev., 30, 1201–1217, doi:10.1016/j.quascirev.2011.02.009, 2011.

Letouzey, J. and Kimura, M.: The Okinawa trough: genesis of a back-arc basin developing along a continental margin, Tectonophysics, 125, 209–230, 1986.

Li, D., Jiang, H., Li, T., and Zhao, M.: Late Holocene paleoenvironmental changes in the southern Okinawa trough inferred from a diatom record, Chin. Sci. Bull., 56, 1131–1138, doi:10.1007/s11434-011-4369-3, 2011.

Lin, S. F., Liew, P. M., and Lai, T. H.: Late Holocene pollen sequence of the Ilan Plain, northeastern Taiwan and its environment and climatic implications, Terr. Atmos. Ocean. Sci., 15, 111–132, 2004.

Lin, S. F., Huang, T. C., Liew, P. M., and Chen, S. H.: A palynological study of environmental changes and their implication for prehistoric settlement in the Ilan Plain, northeastern Taiwan, Veg. Hist. Archaeobot., 16, 127–138, 2007.

Liu, J., Wang, B., and Yang, J.: Forced and internal modes of variability of the East Asian summer monsoon, Clim. Past, 4, 225–233, doi:10.5194/cp-4-225-2008, 2008.

Liu, Y. C.: The importance of Ilan archaeology in Taiwan, Lan J. Hist., 43, 3–27, 2000.

Nakagawa, T., Brugiapaglia, E., Digerfeldt, G., Reille, M., De Beaulieu, J., and Yasuda, Y.: Dense-media separation as a more efficient pollen extraction method for use with organic sediment/deposit samples: comparison with the conventional method, Boreas, 27, 15–24, 1998.

Oppo, D. W., Rosenthal, Y., and Linsley, B. K.: 2000-year-long temperature and hydrology reconstructions from the Indo-Pacific warm pool, Nature, 460, 1113–1116, doi:10.1038/nature08233, 2009.

Qian, W., Hu, Q., Zhu, Y., and Lee, D.-K.: Centennial-scale dry-wet variations in East Asia, Clim. Dynam., 21, 77–89, doi:10.1007/s00382-003-0319-3, 2003.

Reimer, P. J., Brown, T. A., Reimer, R. W.: Discussion: reporting and calibration of post-bomb ^{14}C data, Radiocarbon, 46, 1299–1304, 2004.

Su, H. J.: Studies on the climate and vegetation types of the natural forests in Taiwan (II): altitudinal vegetation zones in relation to temperature gradient, Q. J. Chin. For., 17, 57–73, 1984.

Ter Braak, C. J. and Smilauer, P.: Canoco 4.5: Reference Manual and Canodraw for Windows, User's Guide: software Form Canonical Community Ordination (version 4.5), Microcomputer Power, Ithaca, New York, 2002.

Tsukada, M.: Vegetation in subtropical Formosa during the Pleistocene glaciations and the Holocene, Palaeogeogr. Palaeocl., 3, 49–64, 1967.

Title Page

Abstract | Introduction

Conclusions | References

Tables | Figures

|◄ | ►|

◄ | ►

Back | Close

Full Screen / Esc

Printer-friendly Version

Interactive Discussion

Varma, V., Prange, M., Lamy, F., Merkel, U., and Schulz, M.: Solar-forced shifts of the Southern Hemisphere Westerlies during the Holocene, Clim. Past, 7, 339–347, doi:10.5194/cp-7-339-2011, 2011.

Wan, N.-J., Li, H.-C., Liu, Z.-Q., Yang, H.-Y., Yuan, D.-X., and Chen, Y.-H.: Spatial variations of monsoonal rain in eastern China: instrumental, historic and speleothem records, J. Asian Earth Sci., 40, 1139–1150, doi:10.1016/j.jseaes.2010.10.003, 2011.

Wang, L. C., Lee, T. Q., Chen, S. H., and Wu, J. T.: Diatoms in Liyu Lake, Eastern Taiwan, Taiwania, 55, 228–242, 2010.

Wang, L. C., Wu, J. T., Lee, T. Q., Lee, P. F., and Chen, S. H.: Climate changes inferred from integrated multi-site pollen data in northern Taiwan, J. Asian Earth Sci., 40, 1164–1170, doi:10.1016/j.jseaes.2010.06.003, 2011.

Wang, L.-C., Behling, H., Lee, T.-Q., Li, H.-C., Huh, C.-A., Shiau, L.-J., Chen, S.-H., and Wu, J.-T.: Increased precipitation during the Little Ice Age in northern Taiwan inferred from diatoms and geochemistry in a sediment core from a subalpine lake, J. Paleolimnol., 49, 619–631, doi:10.1007/s10933-013-9679-9, 2013.

Wang, X., Li, Y., Xu, Q., Cao, X., Zhang, L., and Tian, F.: Pollen assemblages from different agricultural units and their spatial distribution in Anyang area, Chin. Sci. Bull., 55, 544–554, doi:10.1007/s11434-009-0480-0, 2010.

Wang, Y., Herzschuh, U., Shumilovskikh, L. S., Mischke, S., Birks, H. J. B., Wischnewski, J., Böhner, J., Schlütz, F., Lehmkuhl, F., Diekmann, B., Wünnemann, B., and Zhang, C.: Quantitative reconstruction of precipitation changes on the NE Tibetan Plateau since the Last Glacial Maximum – extending the concept of pollen source area to pollen-based climate reconstructions from large lakes, Clim. Past, 10, 21–39, doi:10.5194/cp-10-21-2014, 2014.

Weckström, K., Weckström, J., Yliniemi, L.-M., and Korhola, A.: The ecology of Pediastrum (*Chlorophyceae*) in subarctic lakes and their potential as paleobioindicators, J. Paleolimnol., 43, 61–73, doi:10.1007/s10933-009-9314-y, 2010.

Woodruff, J. D., Donnelly, J. P., and Okusu, A.: Exploring typhoon variability over the mid-to-late Holocene: evidence of extreme coastal flooding from Kamikoshiki, Japan, Quaternary Sci. Rev., 28, 1774–1785, doi:10.1016/j.quascirev.2009.02.005, 2009.

Wu, J.-T., Babu, B., Chou, C.-L., and Saraswathi, S. J.: Freshwater Diatom Flora of Taiwan, Biodiversity Research Center, Academia Sinica, Taipei, Taiwan, 2011.

Late Holocene environmental reconstructions in NE Taiwan

L.-C. Wang et al.

Yan, H., Sun, L., Oppo, D. W., Wang, Y., Liu, Z., Xie, Z., Liu, X., and Cheng, W.: South China Sea hydrological changes and Pacific Walker Circulation variations over the last millennium, Nat. Commun., 2, 293, doi:10.1038/ncomms1297, 2011a.

Yan, H., Sun, L., Wang, Y., Huang, W., Qiu, S., and Yang, C.: A record of the Southern Oscillation Index for the past 2000 years from precipitation proxies, Nat. Geosci., 4, 611–614, doi:10.1038/ngeo1231, 2011b.

Yancheva, G., Nowaczyk, N. R., Mingram, J., Dulski, P., Schettler, G., Negendank, J. F. W., Liu, J., Sigman, D. M., Peterson, L. C., and Haug, G. H.: Influence of the intertropical convergence zone on the East Asian monsoon, Nature, 445, 74–77, 2007.

Zhang, P., Cheng, H., Edwards, R. L., Chen, F., Wang, Y., Yang, X., Liu, J., Tan, M., Wang, X., Liu, J., An, C., Dai, Z., Zhou, J., Zhang, D., Jia, J., Jin, L., and Johnson, K. R.: A test of climate, sun, and culture relationships from an 1810-year Chinese cave record, Science, 322, 940–942, doi:10.1126/science.1163965, 2008.

Zheng, W., Wu, B., He, J., and Yu, Y.: The East Asian Summer Monsoon at mid-Holocene: results from PMIP3 simulations, Clim. Past, 9, 453–466, doi:10.5194/cp-9-453-2013, 2013.

Late Holocene environmental reconstructions in NE Taiwan

L.-C. Wang et al.

Title Page

Abstract | Introduction

Conclusions | References

Tables | Figures

|◄ | ►|

◄ | ►

Back | Close

Full Screen / Esc

Printer-friendly Version

Interactive Discussion

Full Screen / Esc

Printer-friendly Version

Interactive Discussion

Table 1. ^{14}C-AMS ages and the calibrated ages of the organic materials in sediment core DH-7B of Dahu Lake.

Depth (cm)	Lab. no.	Materials	^{14}C age (BP)	Calibrated age (AD)*
84.5	NZA 30997	Wood	386 ± 30	1537 ± 95
124.5	NZA 29749	Plant fragments	500 ± 30	1423 ± 25
635.5	NZA 31002	Wood	1319 ± 30	712 ± 60
1248	NZA 29746	Leaf	2125 ± 30	-129 ± 78

* derived from Reimer et al. (2004). $0\,\mathrm{cal\,yr\,BP} = 1950\,\mathrm{AD}$.
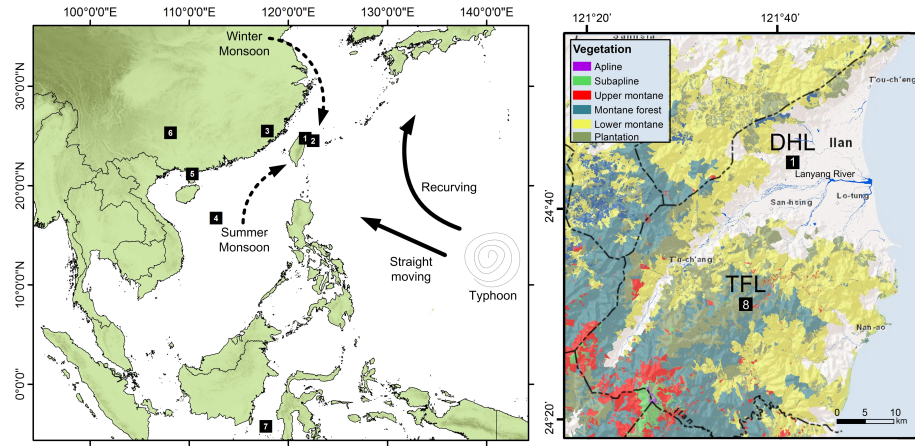
Fig. 1. Major forces affecting precipitations in Taiwan (left panel) and location of Dahu Lake (DHL) with modern vegetation cover (right panel). Locations (black squares) are used for discussions as follow: (1) DHL; (2) South Okinawa Trough; (3) Fujian Province; (4) Cattle Pond, Dongdao Island; (5) Lake Huguang Maa; (6) Dongge Cave; (7) Makassar Strait; (8) Tsuifong Lake (TFL).
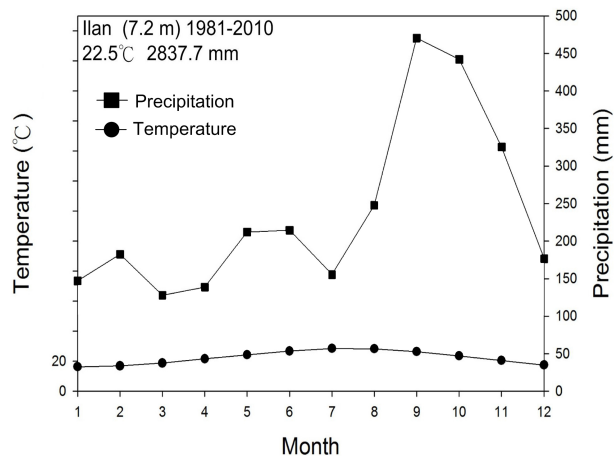
Fig. 2. Mean monthly temperature and precipitation data (1981–2010) collects from the Ilan weather station.
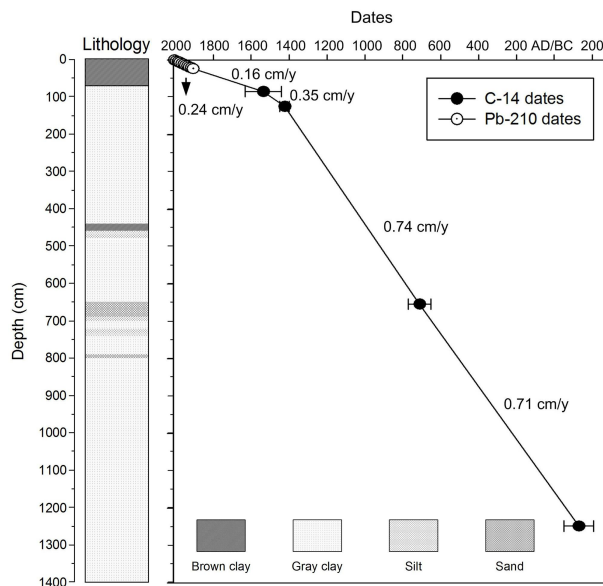
Fig. 3. Lithology and age-depth profile of the studied sediment core from DHL with dates and estimated sedimentation rates.

Fig. 4. Pollen percentage diagrams for selected taxa along with pollen concentrations throughout the sediment core with respect to local pollen zones (LPZ). The percentages of pollen, fern spores, and green algae *Pediastrum* are based on the sum of total pollen. Columns are referred to the samples with low pollen preservation.
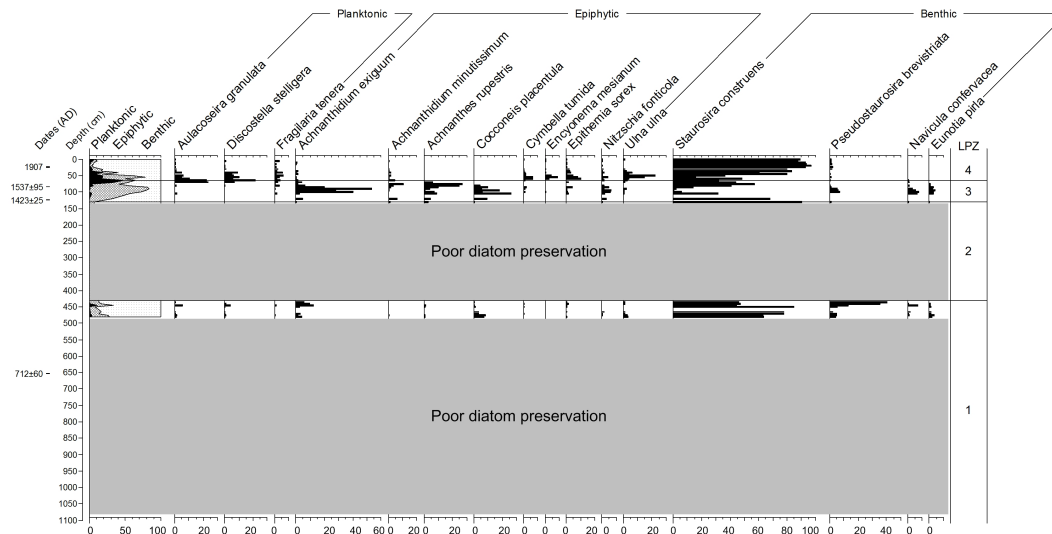
Fig. 5. Sediment profiles of dominant planktonic, epiphytic and benthic diatoms on the basis of pollen zones (LPZ).
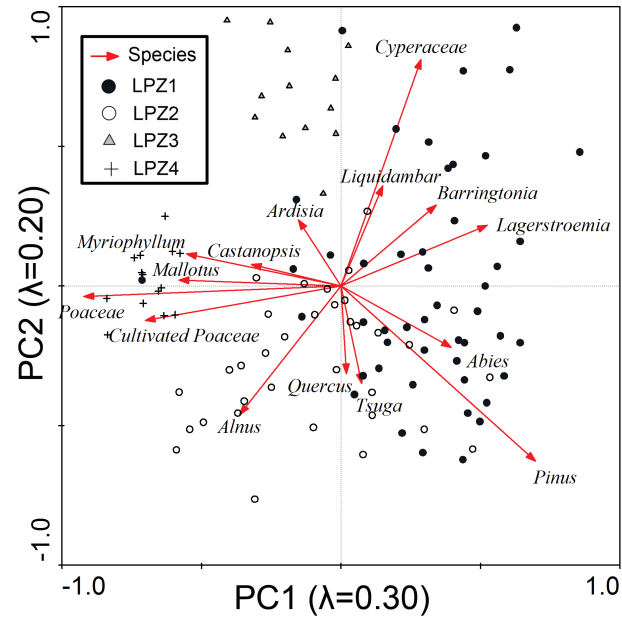
Fig. 6. Results of the principle component analysis of pollen data from DHL and plot of the first axis (PC1) vs. the second axis (PC2).
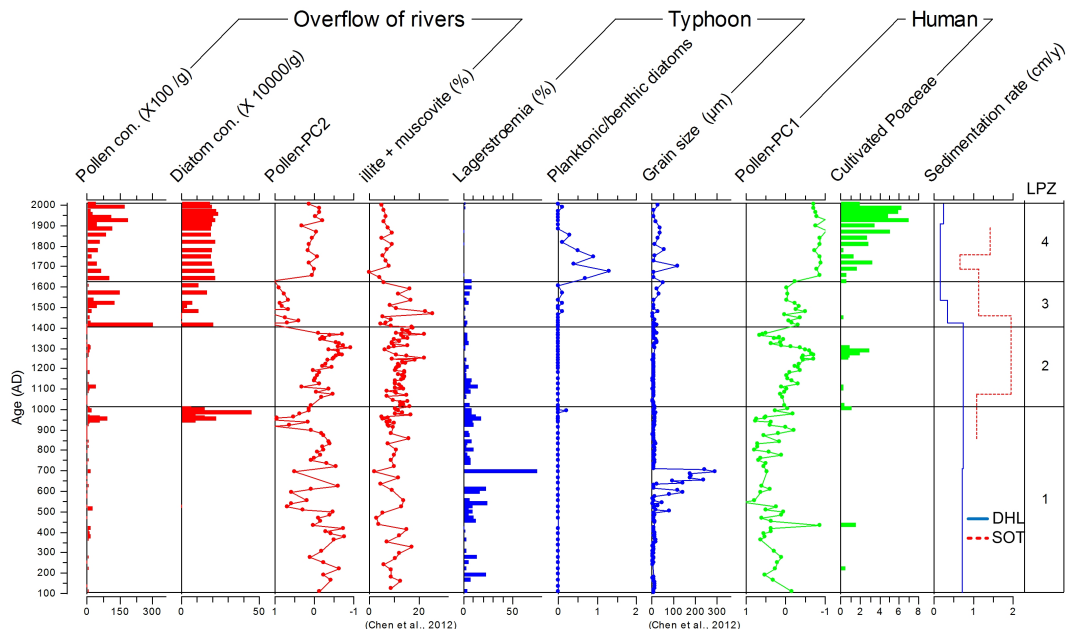
Fig. 7. Pollens and diatoms based reconstruction of flood events, typhoon frequency, and human activities during the last 1900 years. Variations of pollen concentrations, diatom concentrations, Pollen-PC2, the sum of illite and muscovite, percentages of *Lagerstroemia* pollen, ratio of planktonic/benthic diatom, grain size, Pollen PC1, percentage of cultivated Poaceae in DHL, and the sedimentation rate in DHL and SOT on the basis of pollen zones (LPZ).

Discussion Paper | Discussion Paper | Discussion Paper | Discussion Paper | Discussion Paper |

CPD

10, 1977–2009, 2014

Late Holocene environmental reconstructions in NE Taiwan

L.-C. Wang et al.

Title Page

Abstract   Introduction

Conclusions   References

Tables   Figures

|◄   ►|

◄   ►

Back   Close

Full Screen / Esc

Printer-friendly Version

Interactive Discussion
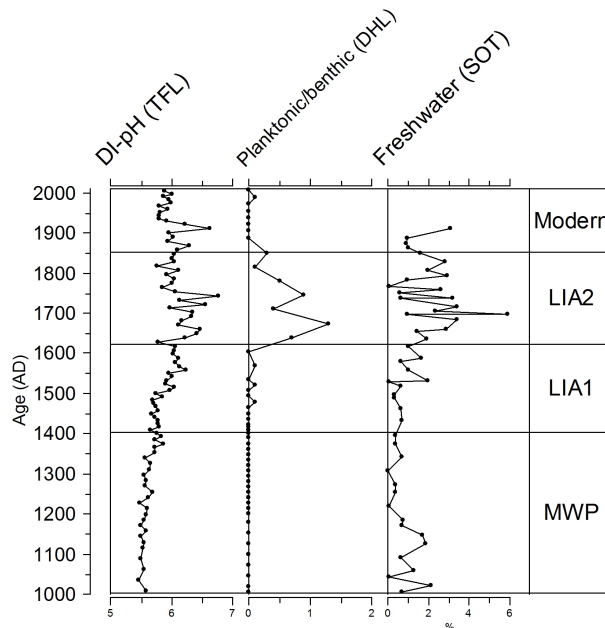
Fig. 8. Variations of diatom-inferred precipitations during the last thousand years in subalpine lake (TFL), lowland lake (DHL), and offshore marine sediments (SOT).
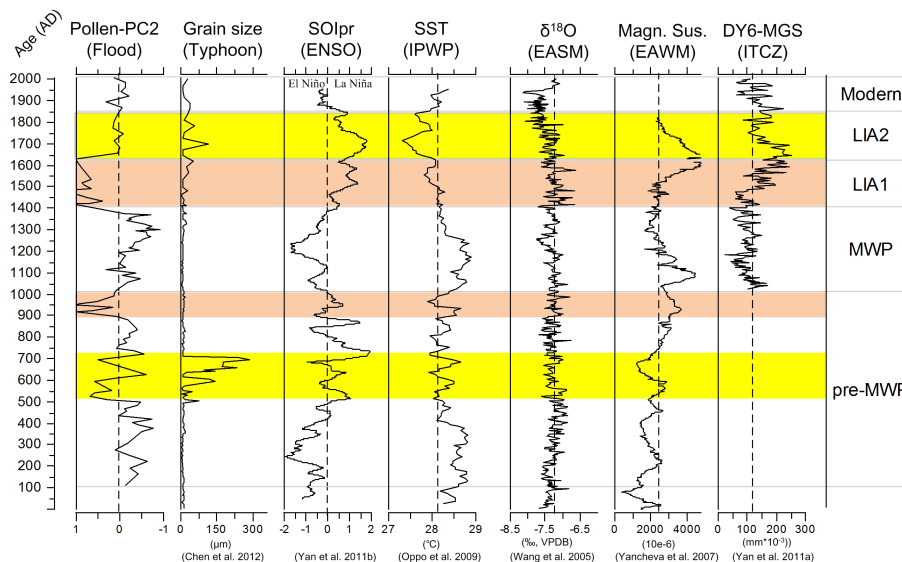
Fig. 9. Variations of flood events and typhoon frequency in Taiwan during the last 1900 years by comparing with reconstructed proxy of ENSO (SOIpr), IPWP (SST of Makassar Strait), East Asia Summer Monsoon (EASM, δ^{18}O speleothem from Dongge Cave), East Asian Winter Monsoon (EAWM, magnetic susceptibility from lake sediments of Lake Huguang Maar), and the shifts of ITCZ (grain size from lake sediments from Cattle Pond, Dongdao Island). Yellow column covers indicate periods with frequently occurring of typhoons, while the red column covers indicate dry periods.

Title Page

Abstract   Introduction

Conclusions   References

Tables   Figures

◀   ▶▎

◀   ▶

Back   Close

Full Screen / Esc

Printer-friendly Version

Interactive Discussion